Three-wave mixing mediated femtosecond pulse compression in BBO

A. Grün,[1,*] Dane R. Austin,[1] Seth L. Cousin,[1] and J. Biegert[1,2]

[1] *ICFO-Institut de Ciencies Fotoniques, Av. Carl Friedrich Gauss, 3, 08860 Castelldefels, Barcelona - Spain*
[2] *Institució Catalana de Recerca i Estudis Avançats, 08010 Barcelona, Spain*
[*] *Corresponding author: alexander.gruen@icfo.es*

Compiled August 5, 2015

Nonlinear pulse compression mediated by three wave mixing is demonstrated for ultrashort Ti:Sapphire pulses in a type II phase matched BBO crystal using noncollinear geometry. 170 µJ pulses at 800 nm with a pulse duration of 74 fs are compressed at their sum frequency to 32 fs with 55 µJ of pulse energy. Experiments and computer simulations demonstrate the potential of sum frequency pulse compression to match the group velocities of the interacting waves to crystals which were initially not considered in the context of nonlinear pulse compression. [redacted]

Nonlinear pulse compression (NPC) via sum-frequency (SF) generation, proposed at the start of the 1990s by Wang and Dragila [1] and Stabinis *et al.* [2], has found a number of successful experimental applications for efficient shortening the SF generated pulses [3–5]. The compression mechanism is based on frequency up-conversion of light pulses in a nonlinear crystal in the case of strong energy exchange and particular conditions of group-velocity mismatch (GVM). Specifically, the crystal has to be chosen such that the group velocities of the NIR pump pulses, v_1 and v_2, and of the sum-frequency generated pulse, v_{SF}, obey the condition $v_1 < v_{SF} < v_2$. In case of strong energy exchange and an appropriate pre-delay between the pump waves, the leading edge of the faster pump pulse and the trailing edge of the slower one are depleted. This way the temporal overlap region of the pump pulses remains narrow resulting in the shortening of the upconverted pulse.

Using a collinear geometry, NPC has been limited to only a few wavelengths due to the lack of suitable uniaxial crystals featuring the appropriate group-velocity mismatch. In the special case of second harmonic generation, effective shortening has only been only demonstrated in Potassium Dihydrogen Phosphate (KDP) crystals which possess the required GVM for Nd-doped lasers emitting near 1.06 µm [3–6]. By matching the interacting wavelengths to the necessary group-velocity condition, nonlinear pulse compression has been shown by generating the sum frequency of 1.3 and 1.95 µm waves in a type II phase-matching β-Barium Borate (BBO) crystal [7]. This crystal has also been used to generate tunable femtosecond pulses within 600-720 nm by mixing pulses from a Nd:glass laser and tunable pulses from a traveling-wave OPA [8]. In order to extend NPC to nonlinear crystals and laser wavelengths which were initially considered inapplicable, one must control the effective group velocities of the interacting pulses in the crystal. To this end, one may adjust the noncollinear phase matching angles and the pulse-front tilt [9]. By suitably selecting these parameters, it is possible to simultaneously achieve phase matching and the required GVM conditions. While tilting the input pulses found successful applications in the context of NPC [10, 11], the idea of a noncollinear interaction [12, 13] has not been realised.

In this letter we show that by use of a noncollinear phase matching geometry, as illustrated in Fig. 1, NPC can be applied to widely used femtosecond Ti:sapphire lasers. As an experimental proof we present compression of sub 100 fs pulses at a 800 nm centre wavelength in a type II BBO crystal. Two orthogonally polarised and

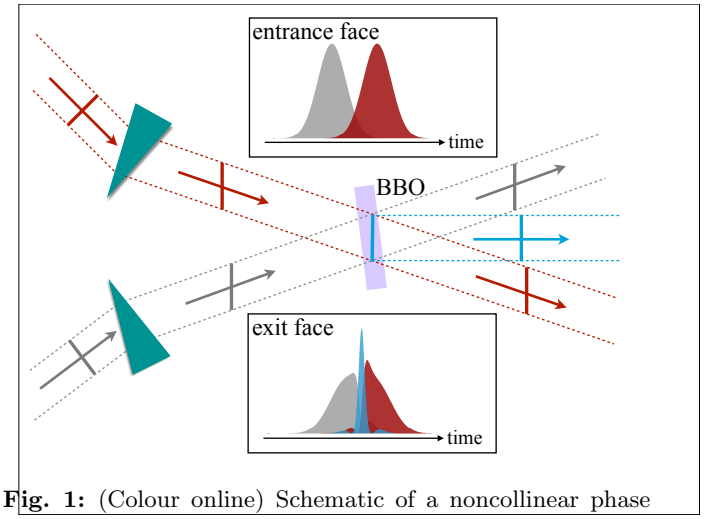

Fig. 1: (Colour online) Schematic of a noncollinear phase matching geometry for SF generation of femtosecond pulses under appropriate conditions of GVM. The ordinary wave is sketched black, the extraordinary wave in red and the SF generated wave in blue. The teal triangles represent angular dispersive elements.

temporally delayed near-infrared pulses intersect in an uniaxial crystal. Figure 2(a) shows the noncollinear angles between the ordinary and extraordinary fundamental wavevectors, $\mathbf{k}_o(\omega)$ and $\mathbf{k}_e(\omega)$, and the SF wavevector, $\mathbf{k}_e(2\omega)$, for type II phasematching in BBO at 785 nm, $\mathbf{k}_o(\omega) + \mathbf{k}_e(\omega) - \mathbf{k}_e(2\omega) = 0$. Requiring the pulse front tilts of the three pulses to be parallel to the SF imposes the following condition on the transverse com-

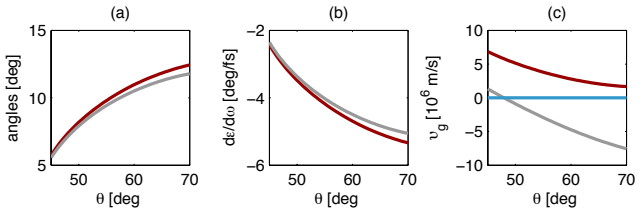

Fig. 2: (Colour online) NPC conditions for femtosecond pulses centred at 800 nm in a type II BBO as a function of the crystal cut angle θ. (a) noncollinear angles, (b) angular dispersions, and (c) group velocities in the frame of reference of the SF pulse (blue). The ordinary and extraordinary components are respectively in grey and red.

ponents of the wavevectors: $\frac{dk_{o,\perp}(\omega)}{d\omega} = \frac{dk_{e,\perp}(\omega)}{d\omega} = 0$ This condition can be satisfied by introducing an angular dispersion $d\alpha/d\lambda$ for the ordinary and extraordinary components. The required angular dispersion is shown in Fig. 2(b). Note that the pulse front tilt φ, the angle between the pulse front and the phase front, is related to the angular dispersion by $\tan\varphi = -\lambda_0 \frac{d\alpha}{d\lambda}$, where λ_0 is the centre wavelength [14]. The resulting group velocities $\upsilon_i = \left[\frac{d\omega}{dk_{i,\parallel}(\omega)}\right]^{-1}$ are shown relative to that of the sum frequency in Fig. 2(c). Note that the effective interaction volumes of this technique are limited to the region of geometrical overlap of the pump beams which is not an issue for femtosecond pulses as the interaction length is in the order of 100 to 400 µm but cannot be neglected for picosecond pulses.

The experiments were performed in a 250 µm thick type II phase matching BBO crystal angle tuned for $\theta = 55°$, by mixing the apertured pulses from the output of a Ti:sapphire laser providing nearly Fourier transform-limited pulses with 74 fs duration centred at 785nm and e 3 s ed

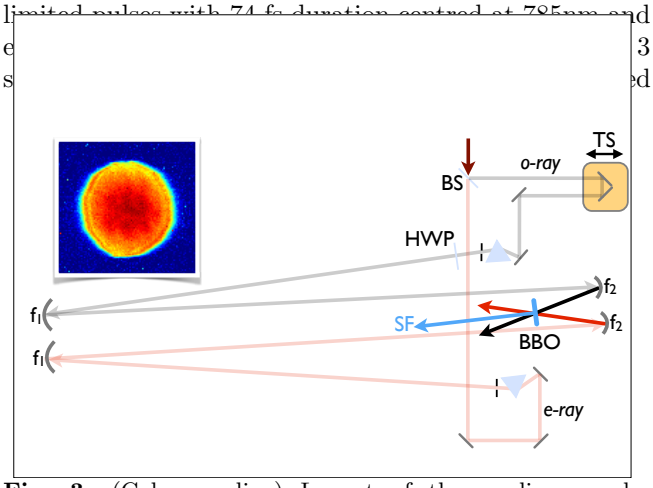

Fig. 3: (Colour online) Layout of the nonlinear pulse compression setup. BS, beamsplitter; TS, translation stage; HWP, half-wave plate; f_i, curved mirrors; SF, sum-frequency generated wave. The inset shows the beam profile in the crystal plane.

Ti:sapphire pulse was split by a 50:50 beamsplitter (BS). The reflected part is delayed through a stage (TS) and passed through a half-wave plate (HWP) which was placed after the prism. For positive delay the σ-polarised wave enters first into the crystal. The crystal is oriented in such a way that the ordinary axis, where the pulse has a lower group velocity, aligns with the σ-polarised wave. The equilateral prisms (Thorlabs 853) are made out of crown glass (F2), introducing a pulse-front tilt of ∼2.6° and ∼3° at incident angles of 60° and 55° for the ordinary and extraordinary arms respectively. We used protected reflective curved mirrors instead of lenses to avoid unwanted nonlinear effects. The two pairs of concave mirrors (r=-1500 mm and r=-250 mm) formed a downsizing telescope providing a lateral magnification of 1/6. The combination of prism and telescope finally induces a pulse-front tilt of ∼16° on the π-polarised pulse and ∼18° on the σ-polarised pulse outside the BBO crystal which translates to a pulse-front tilt of ∼9.5° and ∼10° respectively inside the crystal. Since the NPC dynamics are very intensity sensitive, a flat top beam profile is desired, and a portion of the beam with near-uniform intensity was selected by placing an iris directly after the prisms into each beam path. The pulse energy in each beam was 200 µJ corresponding to a total intensity of 4 TW/cm^2 at the entrance of the BBO crystal with an iris aperture of 2.5 mm. Diffraction rings are not an issue because the telescopes relay the planes of the prisms onto the crystal as can be seen in the inset of Fig. 3. For the temporal characterisation of the sum-frequency generated pulses we used frequency-resolved optical gating (FROG) [15, 16] based on self-diffraction (SD) in a 100 µm thick sapphire plate.

The retrieved pulse duration at full width at half maximum and the energy of the SF pulse as a function of pre-delay between the pump pulses are reported in Fig. 4. For pre-delays ranging between -40 fs and 40 fs (approximately half the duration of a fundamental frequency pulse) moderate pulse compression was observed. A large to complete superposition of the pump pulses at the beginning, i.e. a long temporal overlap region, leaded to a strong energy transfer and thus high SF pulse energies. The overall pump depletion, in contrast to solely depletion of the edges, reduced the temporal compres-

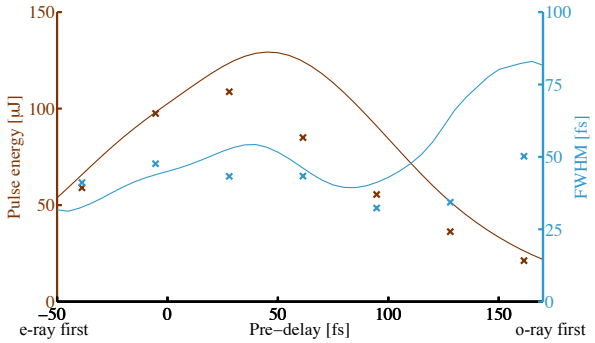

Fig. 4: (Colour online) SF pulse energy (brown) and pulse width (blue) as a function of the pump pulse pre-delay. Crosses represent experimental data, continuous lines represent simulation results.

sion efficiency. In this range the maximum conversion efficiency of 27% was achieved for a pre-delay of about ∼30 fs between the initial pump pulses. The SF pulse energy was 108 µJ at this point with a pulse duration of 40 fs. For pre-delays below -40 fs and exceeding 140 fs only the tails of the pump pulses overlapped at the start respectively at the exit of the BBO, which translated in a very weak interaction. Considerable nonlinear pulse compression was observed for pre-delays ranging between 90-140 fs, i.e. when the o-ray entered the crystal with more than one pulse duration in advance of the e-ray. In this situation the e-ray could completely "catch up" to the o-ray in the crystal while the strong depletion of the NIR provided a very short temporal overlap region over the entire propagation length. The best compression occurs with a delay of 90 fs, at which 30 fs pulses of 50 µJ energy are produced.

Figure 5(a) shows the corresponding measured spectra and Fig. 5(b) the retrieved temporal intensities for a restricted range of pre-delays which is of particular interest. Substantial spectral broadening, see Fig. 5(a), could be observed for pre-delays ranging between -40 fs and 40 fs.

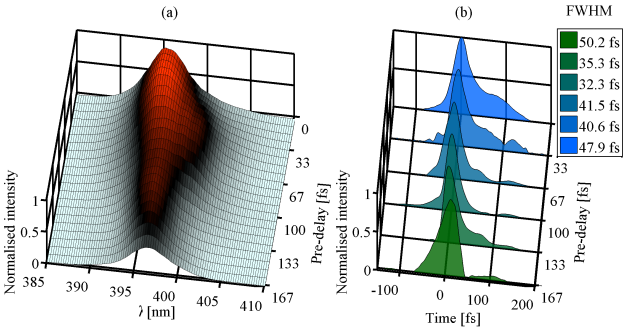

Fig. 5: (Colour online) (a) Measured sum-frequency generated spectra and (b) reconstructed temporal intensity as a function of the pre-delay.

The shortest SF pulse is presented in more detail in Fig. 6. The measured SD-FROG trace and the FROG trace of the retrieved pulse can be seen in Fig. 6(a) and (b). The reconstructed spectrum and the spectral phase are shown Fig. 6(c). Figure 6(d) finally shows the temporal intensity of the retrieved 32.2 fs (FWHM) pulse (blue) together with the reconstruction of the initial NIR 74 fs (FWHM) pulse (red). Also shown in Fig. 6(d) is the reconstructed 67 fs (FWHM) pulse generated by SF mixing the aforementioned NIR pulse in a 30 µm thin BBO crystal (dashed line), where no compression was expected. This pulse was twice as long as the compressed SF pulse generated in the 250 µm long BBO crystal.

The experimental results have been compared with computer simulations performed by numerically solving the set of nonlinear coupled equations for the interacting pulses taking into account both group-velocity mismatch and group-velocity dispersion effects. A detailed description of the theoretical model was presented pre-

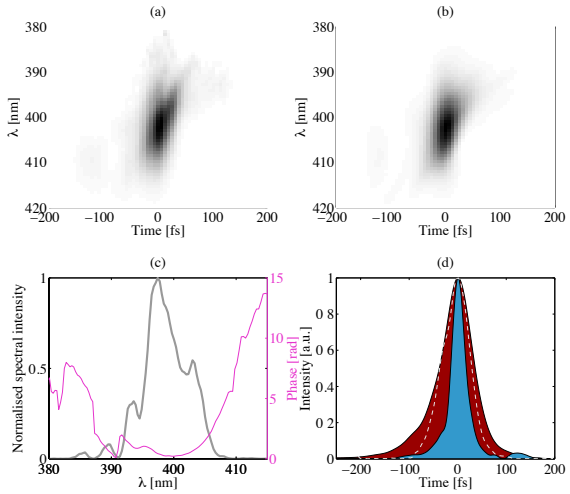

Fig. 6: (Colour online) SF pulse. (a) Measured FROG trace, (b) reconstructed FROG trace, (c) reconstructed spectrum and spectral phase, and (d) reconstructed temporal intensity shape of the SF pulse generated in a 250 µm thick (blue) and in a 30 µm thick (dashed line) BBO crystal and of the initial NIR pulse (red).

viously by Biegert *et al.* [13]. Thermal effects, self-phase modulation and two-photon absorption have been neglected. The wavevectors contain the angular dispersion and the noncollinear angles calculated for a crystal cut angle of 55°. As initial pump pulses we used the full reconstruction of a pulse measured with second harmonic generation FROG. Figure 4 shows that the numerical results are in good agreement with the experimental results. We found that especially long pulse tails can trigger the back-conversion of the ultrashort SF generated wave to the fundamental wave in an unfavourable way, resulting in a reduced conversion efficiency and longer SF pulses compared to perfect Gaussian input pulses.

In conclusion, we have demonstrated efficient nonlinear pulse compression by sum-frequency mixing ultrashort pulses from a Ti:sapphire amplifier laser using a noncollinear setup. This is of interest, because there is no crystal that can be used for nonlinear pulse compression at wavelengths near 800 nm in a collinear geometry. An important advantage of the presented scheme, compared to a collinear three-wave interaction with tilted input pulses, is that the required energy front tilts are approximately three times smaller and that the sum-frequency generated pulses emerge untilted.

References

1. Y. Wang and R. Dragila, "Efficient conversion of picosecond laser pulses into second-harmonic frequency using group-velocity dispersion," Phys. Rev. A **41**, 5645–5649 (1990).
2. A. Stabinis, G. Valiulis, and E. Ibragimov, "Effective sum frequency pulse compression in nonlinear crystals," Optics Communications **86**, 301 – 306 (1991).

3. Y. Wang and B. Luther-Davies, "Frequency-doubling pulse compressor for picosecond high-power neodymium laser pulses," Opt. Lett. **17**, 1459–1461 (1992).
4. P. Heinz, A. Laubereau, A. Dubietis, and A. Piskarskas., "Fiberless two-step parametric compression of sub-picosecond laser pulses," Lith. J.Phys. **33**, 314 (1993).
5. A. Umbrasas, J.-C. Diels, J. Jacob, G. Valiulis, and A. Piskarskas, "Generation of femtosecond pulses through second-harmonic compression of the output of a nd:yag laser," Opt. Lett. **20**, 2228–2230 (1995).
6. C. Y. Chien, G. Korn, J. S. Coe, J. Squier, G. Mourou, and R. S. Craxton, "Highly efficient second-harmonic generation of ultraintense nd:glass laser pulses," Opt. Lett. **20**, 353–355 (1995).
7. M. Nisoli, S. D. Silvestri, and O. Svelto, "Generation of high energy 10 fs pulses by a new pulse compression technique," Applied Physics Letters **68**, 2793–2795 (1996).
8. R. Danielius, A. Piskarskas, P. D. Trapani, A. Andreoni, C. Solcia, and P. Foggi, "Matching of group velocities by spatial walk-off in collinear three-wave interaction with tilted pulses," Opt. Lett. **21**, 973–975 (1996).
9. A. V. Smith, "Group-velocity-matched three-wave mixing in birefringent crystals," Opt. Lett. **26**, 719–721 (2001).
10. A. Dubietis, G. Valiulis, G. Tamošauskas, R. Danielius, and A. Piskarskas, "Nonlinear second-harmonic pulse compression with tilted pulses," Opt. Lett. **22**, 1071–1073 (1997).
11. A. Dubietis, G. Valiulis, G. Tamošauskas, R. Danielius, and A. Piskarskas, "Nonlinear pulse compression in the ultraviolet," Optics Communications **144**, 55 – 59 (1997).
12. T. R. Zhang, H. R. Choo, and M. C. Downer, "Phase and group velocity matching for second harmonic generation of femtosecond pulses," Appl. Opt. **29**, 3927–3933 (1990).
13. J. Biegert and J.-C. Diels, "Compression of pulses of a few optical cycles through harmonic generation," J. Opt. Soc. Am. B **18**, 1218–1226 (2001).
14. Z. Bor, B. Racz, G. Szabo, M. Hilbert, and H. A. Hazim, "Femtosecond pulse front tilt caused by angular dispersion," Optical Engineering **32**, 2501–2504 (1993).
15. D. Kane and R. Trebino, "Characterization of arbitrary femtosecond pulses using frequency-resolved optical gating," Quantum Electronics, IEEE Journal of **29**, 571 – 579 (1993).
16. K. W. DeLong, R. Trebino, and D. J. Kane, "Comparison of ultrashort-pulse frequency-resolved-optical-gating traces for three common beam geometries," J. Opt. Soc. Am. B **11**, 1595–1608 (1994).